BAOBABS ON KUBU ISLAND, BOTSWANA – A DENDROCHRONOLOGICAL MULTI-PARAMETER STUDY USING RING WIDTH AND STABLE ISOTOPES ($\delta^{13}C$, $\delta^{18}O$)

Franziska Slotta, Gerhard Helle, Karl-Uwe Heussner,
Elisha Shemang and Frank Riedel

With 10 figures and 2 tables
Received 01 July 2015 · Accepted 08 January 2016

Summary: According to the Intergovernmental Panel on Climate Change (IPCC), all of Africa is very likely to warm up more than the global average during this century. Especially (semi-)arid regions are expected to experience particularly high warming and possibly catastrophic droughts. However, assessments of the impacts of climate change on these regions are currently impeded by a lack of transregional high temporal resolution proxy data for the African continent. Baobab trees are widely distributed in (semi-)arid Africa and can reach ages of up to 2000 years. This pilot study was aimed at investigating African baobabs, *Adansonia* spp., from a site in Botswana using multiple dendroclimatological methods. Increment cores from 16 individual baobabs growing on Kubu Island (20°53' S, 25°49' E), a granite pluton located in the Kalahari, were collected in June 2011 to test for annual growth and the species' utility for palaeoclimatic studies. Due to the particular wood fabric and relatively high water content, baobab increment cores were packed in air-tight opaque tubes and stored in a freezer to prevent drying and mould formation. The complicated wood anatomical structure was found to be analysed best using a microscope with incident UV light, allowing tree-ring boundaries to be distinguished. Nonetheless, potential differences in individual site conditions, as well as diverse tree ages, caused conventional dendrochronological crossdating to fail. Missing and false tree rings could be identified due to the strong relationship between tree-ring width and annual precipitation amount allowing the development of a preliminary 50 year-long baobab chronology (1960–2009). Subsequently, stable carbon and oxygen isotope analyses revealed significant correlations of $\Delta^{13}C$ and $\delta^{18}O$ of tree rings with climate data. Year-to-year isotope variability and trends were found to be in good agreement with established models of fractionation. Intrinsic water-use efficiency has mainly increased over the study period (2–30 %). Despite the demonstrated high potential of African baobabs as a valuable high-resolution climate archive, we conclude that more dendrochronological calibration studies are required at various sites in southern Africa. Furthermore, ecophysiological monitoring of climate and stable isotope signal transfer from the atmosphere, through soil and leaves into the tree rings is necessary to fully understand tree-ring formation and climate response of the African baobab.

Zusammenfassung: Laut Weltklimarat (Intergovernmental Panel on Climate Change, IPCC) wird Afrika sehr wahrscheinlich eine Erwärmung erfahren, die über dem globalen Mittel liegen wird. Speziell aride Gebiete sind durch eine hohe Erwärmung und mögliche katastrophale Dürren gefährdet. Den Einschätzungen der Auswirkungen des Klimawandels auf diese Regionen steht aber derzeit ein großer Mangel an überregionalen, zeitlich hochaufgelösten und präzise datierten Proxy-Datenreihen für den afrikanischen Kontinent entgegen. Baobabs sind im (semi-)ariden Afrika weit verbreitet und können bis zu 2000 Jahre alt werden. Das Ziel dieser Pilotstudie war es, Afrikanische Baobabs, *Adansonia* spp., von einem Standort in Botsuana mit verschiedenen dendrochronologischen Methoden zu untersuchen. Im Juni 2011 wurden 16 Baobabs auf Kubu Island (20°53‘ S, 25°49‘ E), einem Granitpluton in der Kalahari Botsuanas, Zuwachsbohrkerne entnommen, um zu testen, ob es sich bei den Zuwachszonen der Baobabs um Jahrringe handelt und, um ihre Nutzbarkeit für Paläo-Klimastudien zu untersuchen. Aufgrund ihrer besonderen Holzstruktur und dem relativ hohen Wassergehalt wurden die Zuwachsbohrkerne in luftdichte, lichtundurchlässige Röhren verpackt und so schnell wie möglich eingefroren, um Austrocknung und Schimmelbildung zu verhindern. Die komplizierte Holzanatomie lässt sich am besten mit einem UV-Licht-Mikroskop analysieren, das die Differenzierung der Jahrringgrenzen ermöglicht. Trotzdem führten potentielle Standort- und Altersunterschiede dazu, dass die Proben nicht auf konventionelle Art kreuzdatiert werden konnten. Der stark ausgeprägte Zusammenhang zwischen Jahrringbreite und Jahresniederschlag ermöglichte es aber, fehlende und falsche Jahrringe zu identifizieren und so eine vorläufige 50 Jahre lange Baobab-Chronologie (1960–2009) zu erstellen. Die anschließende Analyse stabiler Kohlenstoff- und Sauerstoffisotope ergab signifikante Korrelationen von $\Delta^{13}C$ und $\delta^{18}O$ der Jahrringe mit Klimadaten. Die jährliche Isotopenvariabilität und die Trends der Isotope sind im Einklang mit anerkannten Fraktionierungs-Modellen. Die intrinsische Wassernutzungseffizienz hat sich über den Untersuchungszeitraum überwiegend verbessert (2–30 %). Trotz des demonstrierten großen Potentials der Afrikanischen Baobabs als zukünftiges hoch-aufgelöstes Klimaarchiv kommen wir zu dem Schluss, dass es weiterer dendrochronologischer Kalibrierungsstudien an unterschiedlichen Standorten im südlichen Afrika bedarf. Darüber hinaus ist ein ökophysiologisches Monitoring des Transfers von Klimasignalen und stabilen Isotopen aus der Atmosphäre durch den Boden und die Blätter in die Jahrringe erforderlich, um die Jahrringbildung und die Klimareaktion der Afrikanischen Baobabs vollständig zu verstehen.

Keywords: Southern Africa, palaeoclimatology, dendrochronology, Baobab, *Adansonia* spp., UV light

https://doi.org/10.3112/erdkunde.2017.01.02 ISSN 0014-0015 http://www.erdkunde.uni-bonn.de

1 Introduction

1.1 The need for climate proxies in southern Africa

Despite the awareness of tropical dry regions' vulnerability to climate change, i.e. the shifting towards more arid conditions and thus an increasing "climatological risk of desertification" (Spinoni et al. 2015), the prediction of related effects at a regional and transregional scale remains challenging. High resolution continuous climate records are less abundant in the southern hemisphere than north of the equator (Mayewski et al. 2004; Neukom and Gergis 2012), with a particular lack for interior southern Africa (Maslin and Christensen 2007). As a consequence, current models have significant systematic errors in and around Africa, whose effects on climate projections are difficult to assess (IPCC 2007, 2013).

Since climate patterns vary at regional scale (Nicholson and Kim 1997), insufficient data from a region can lead to inadequate or misleading interpretations (Sletten et al. 2013). A screening for continuous, high temporal resolution palaeoclimate records in the southern hemisphere suitable for palaeoclimate reconstructions by Neukom and Gergis (2012) revealed only 14 data sets for the entire African subcontinent (7 marine coral records, 2 tree-ring chronologies, 5 historical documents). None of these records extends further than 1500 A.D. (Neukom and Gergis 2012). Nonetheless, these available proxies have been used to reconstruct decadal-scale variations in summer and winter precipitation for southern Africa over the last 200 years (Neukom et al. 2013). A well-developed understanding of the natural variability underlying global climate change will require more and better records in southern Africa (Sletten et al. 2013).

The study of multi-centennial trees, archiving annual to seasonal climate signals, appears to be the most promising approach for studying the last millennial climate on the African continent. Relative to other comparable natural climate archives (i.e. lacustrine, marine and stalagmite records), woody plants with clear annual rings are uniquely widespread in areas where the local climate imposes a single dormant season per year (Hughes 2011), as it is the case for interior southern Africa. However, dendrochronology in the tropics is seriously hampered by the complex ring anatomy of many species, including the occurrence of indistinct growth rings (Détienne 1989; Sass et al. 1995), growth ring anomalies (Priya and Bhat 1998; Tarhule and Hughes 2002; Heinrich and Banks 2006) leading to problems in crossdating (Belingard et al. 1996; February and Stock 1998) and in correlation with climatic data (February and Gagen 2003). Nevertheless, species such as the Clanwilliam cedar, *Widdringtonia cedarbergensis* (Dunwiddie and Lamarche 1980), the Bleedwood tree, commonly also known as Mukwa tree or Kiaat, *Pterocarpus angolensis* (Stahle et al. 1999; Fichtler et al. 2004) and the Msasa tree, *Brachystegia spiciformis*, (Trouet et al. 2001; Trouet et al. 2006; Trouet et al. 2010) have proven their value for dendrochronological studies in southern African arid regions. The currently longest chronology of *B. spiciformis* from central Zambia, covers around 150 years (Trouet et al. 2010), the tree-ring width chronology of *P. angolensis* from western Zimbabwe is around 200 years long (Therrell et al. 2006), and the longest tree-ring record of *W. cedarbergensis* from south western South Africa dates back to the mid 16th century (Dunwiddie and Lamarche 1980). In addition to ring widths, tree rings also provide climatic information by the ratios of stable isotopes incorporated in their cellulose. The ratios are controlled by a number of external factors (e.g. temperature, relative humidity) and internal factors (e.g. stomatal conductance, photosynthetic rate) that are reasonably well understood (Farquhar et al. 1982; Roden et al. 2000; Helle and Schleser 2004; Mccarroll and Loader 2004; Treydte et al. 2004; Seibt et al. 2008).

The present study was aimed at investigating the African baobabs, *Adansonia digitata* and *A. kilima*, as potential new high-resolution climate archives for historical times, since they are widely distributed in (semi-)arid Africa (Wickens 1979) and can reach ages of almost 2000 years (Patrut et al. 2013).

1.2 The African baobabs *(Adansonia digitata / A. kilima)*

With their enormous size and their distinctive and often bizarre appearance, the African baobabs have attracted the attention of many researchers of various disciplines (Adanson 1759; Livingstone 1868; Pock Tsy et al. 2009; Riedel et al. 2012). The species are geographically distributed in (semi-)arid and partly semi-humid tropical Africa south the Sahara (Wickens 1979; Fig. 1a).

Adansonia digitata shows a wide range of phenotypic variability regarding inter alia stem height, bark colour, flowering times, leaf and fruit morphology, suggesting numerous local types. A recent phylogenetic study identified a new species, *A. kilima*, that co-exists with *A. digitata* in southeastern and southern Africa (Pettigrew et al. 2012). Baobabs are typically present in areas with 150–800 mm average annual rainfall and from altitudinal ranges close to sea level to about 1.500 m (Fenner 1980; Wickens 1982; Wickens and Lowe 2008; personal observation). They grow either solitary, in small groups or dense clumps with a closed or almost closed canopy (Wilson 1988). As stem succulents, baobabs store huge amounts of water within their trunk. The wood is soft and weak with a very high parenchyma content. The typical large stem diameters and stout branches of wide roundish crowns might therefore be a biomechanical compromise to ensure inherent stability (Chapotin et al. 2006b). Physiological processes such as leaf flushing and buffering daily water deficits require stored water and lead to diurnal and seasonal girth changes of the trunks (Guy 1970; Fenner 1980; Chapotin et al. 2006a, 2006c). The longevity of the African baobabs has long been doubted by some authors, but radiocarbon dating reveal the ages of baobabs from different sites reaching 1000 years up to 2000 years (Swart 1963; Patrut et al. 2007; Patrut et al. 2013; Riedel et al. 2014); that makes them the longest living angiosperms. Although *Adansonia* spp. are deciduous species, shedding their leaves at the end of the rainy season, their usability for dendrochronological and palaeoclimatic studies is questioned. A secure identification of annual growth rings is often complicated by its complex wood anatomy. Owing to harsh environmental conditions, missing and false rings make dendrochronological crossdating difficult. By analysing their radiocarbon content Robertson et al. (2006) identified baobab wood growth rings as being annual. They suggested that high-resolution information about past climates may be obtained by analysing the carbon isotope values from the wood samples. Indeed, a first successful rainfall reconstruction for northeastern South Africa, based on carbon isotope analysis of baobab trees, has only recently proven centennial and decadal scale variability over the last 1000 years (Woodborne et al. 2015).

In this study we introduce a well elaborated guideline for sample preparation and visual identification of growth rings for dendrochronological and stable isotope investigations on baobabs. The question of the annual nature of baobab tree rings will be evaluated for a site in the Kalahari (Botswana) and discussed with respect to the main climatological and environmental drivers of baobab wood growth, ^{13}C discrimination, and intrinsic water-use efficiency.

2 Material and methods

2.1 Study site and sampling

The study was carried out on Kubu Island (20°53' S, 25°49' E), a granite pluton located in the Kalahari, Botswana (Fig. 1b). Kubu Island is situated at the edge of Sua Pan that forms together with Ntwetwe Pan the basin of the palaeolake Makgadikgadi (Cooke 1979). Kubu Island has an

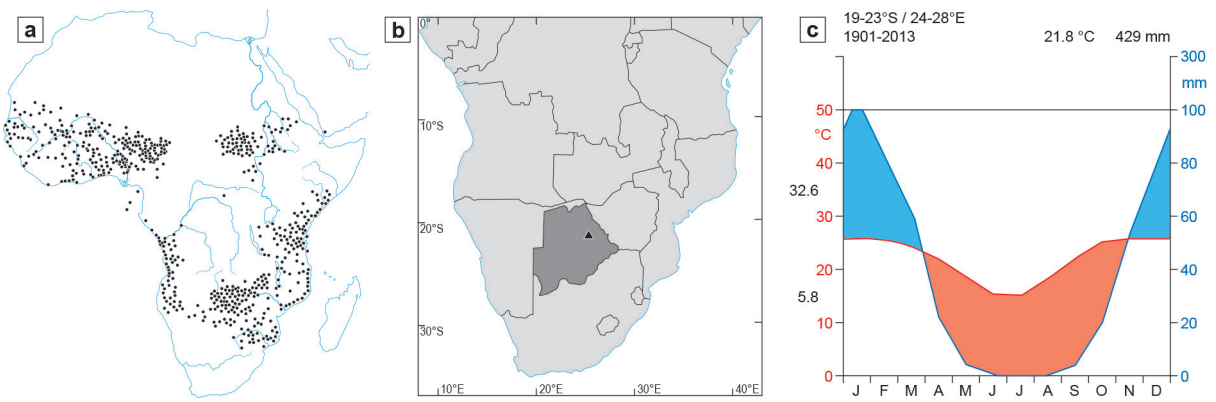

Fig. 1: Context of the study site. (a) Geographical distribution of *Adansonia* spp. over Africa (Wickens 1979). (b) Location of the study site, Kubu Island, Botswana (for details see Riedel et al. 2012). (c) Climate diagram, following Walter and Lieth (1960), for the area around Kubu Island. Daily maximum average temperature of the hottest month and daily minimum average temperature of the coldest month are given in black at the left margin of the diagram (data source: climexp.knmi.nl, CRU TS3.22).

area of about 1.7 km² and reaches elevations of 904–926 m a.s.l. (Riedel et al. 2012). The climate is characterised by highly variable precipitation with an annual mean of 429 mm (203–776 mm), falling mainly from October to April (Fig. 1c). The evaporation rate exceeds 8 to 10 times the precipitation amount (Hitchcock and Nangati 2000). A low level of paedogenesis on Kubu Island leads to a vegetation dominated by grasses and shrubs. Besides some smaller tree and shrub species, the landscape is characterised by more than 100 baobabs (Fig. 2, Tab. 1), presumably *A. digitata*, although we cannot tell the species with certainty. Due to their shallow root system (Fenner 1980), baobabs on Kubu Island do not have access to groundwater and rely completely on precipitation events. The sampling strategy included apparently healthy individuals of all age classes (circumferences ranging from 1.1 to 9.7 m) and mostly without visible mechanical injuries. None of the trees showed characteristic damages caused by elephants. A total of 16 individual baobab trees were sampled in June 2011 and 20 increment cores of 5 mm in diameter and 80 cm in length were obtained, i.e. some of the trees were sampled twice, orientated perpendicular, to check for possible differences in radial growth. All core samples were put into airtight tubes and kept in a freezer as soon as possible to prevent drying and mould formation.

Fig. 2: Baobab tree sampled on Kubu Island (*Bao17*), approximately 15 m high

2.2 Meteorological data

The nearest meteorological stations Letlhakane, Orapa and Nata are located 63 km, 69 km southwest and 85 km northeast from Kubu Island, respectively. Their meteorological records are rather short, reaching back to 1983 (Letlhakane), 1968 (Orapa) or 1959 (Nata). To obtain a robust regional climate signal for the area around Kubu Island, a larger grid area (19–23°S, 24–28°E) is required. The KNMI Climate Explorer (www.climexp.knmi.nl) offers inter alia free global interpolated grid data sets from various providers for climate quantities such as temperature, precipitation, cloud cover etc. with a resolution of up to 0.5° latitude and longitude (see Trouet and Van Oldenborgh 2013 for guidance). In this study, data provided by the Climate Research Unit of the University of East Anglia (CRU TS3.10.01, TS3.22) was used for correlations between tree-ring widths and climate data. The modelled precipitation data and the instrumental records were compared for statistical similarity and found with good correlation (CRU vs. Letlhakane: $r = 0.74$, $p < 0.0001$; CRU vs. Orapa: $r = 0.83$, $p < 0.0001$; CRU vs. Nata: $r = 0.85$, $p < 0.0001$).

2.3 Ring-width measurements

The wood core samples were remoistened with purified water to prevent drying related shrinking of the material. To study the wood anatomical details, the samples were cut perpendicular to the vessel diameters, i.e. perpendicular to longitudinal stem growth. The wood increment cores taken and preserved were too soft for clamping and cutting with a microtome and were thus cut by hand with a razor blade. Different light sources (reflected light, transmitted light, UV light: 365 nm) were tested to maximise the amount of visible information obtained from the cores. Photographs of the cores were taken under UV light (microscope: Nikon SMZ800, camera head: Nikon DIGITAL SIGHT

Tab. 1: Location, size and phenological state of the sampled baobab trees.

Sample	Coordinates (°S / °E)	Altitude (m a.s.l)	Tree height (m) *	Girth (m)	Leaves	Fruits
Bao1, 2	20.893060 / 25.827032	915	12.5	6.0	-	+
Bao3	20.889768 / 25.830724	904	6.0	6.0	+	-
Bao4, 5	20.889518 / 25.829827	912	9.5	7.4	-	-
Bao6, 7	20.889518 / 25.829828	913	9.5	9.7	+	-
Bao8, 9	20.889378 / 25.828025	902	8.0	6.0	+	-
Bao10	20.892997 / 25.823362	910	11.0	2.7	-	-
Bao11	20.892997 / 25.823362	911	7.5	1.3	-	-
Bao14	20.892997 / 25.823362	910	13.0	4.0	-	-
Bao15	20.892997 / 25.823362	910	9.5	7.0	-	-
Bao17	20.892997 / 25.823362	910	15.0	7.0	-	++
Bao19	20.893426 / 25.823139	909	10.0	6.8	-	-
Bao20	20.894409 / 25.826583	914	6.0	2.5	+	+
Bao21	20.894409 / 25.826583	914	7.0	5.5	-	-
Bao22	20.894080 / 25.826888	907	4.5	1.1	-	-
Bao23	20.894080 / 25.826888	907	6.0	2.3	-	-
Bao24	20.894080 / 25.826888	907	9.5	6.5	-	-

height ± 0.5 m, girth ± 0.1 m, without leaves/fruits (-), a few leaves/up to 10 fruits (+), many leaves/more than 10 fruits (++), *determined from photograph

DS-Vi1, TV Lens 0.55x DS, control unit: DS-U2, program: Nikon NIS-Elements, version 3.22.00 © 1991–2010 Laboratory Image, 1600 x 1200 pixels) and merged accurately (Adobe Photoshop CS2, version 9.0.2 © 1990–2005 Adobe Systems Incorporated) for tree-ring width measurements. Some twisted cores had to be rotated during photography in order to maintain the transversal view. In these cases, care was taken whilst photograph merging to ensure the exact distances between the tree-ring boundaries. A subset of 4 cores was dried for a comparative study of the effects of shrinkage on tree-ring width sequences. Air dried samples were glued on conventional wooden sample holders with the transverse core surface facing up. After preparing the surface with a microtome, the core samples were cleaned from loose material via compressed air and then scanned. A special image analysis system (WinDENDRO™ © 1989–2009 Regent Instruments Canada Inc.) was used, enabling precise and efficient measurement of tree-ring widths and related parameters from high quality digital images. Compared to the conventional surveyor table systems, image based measurements allow an easy review and correction of individual rings, which is especially useful for little studied and complex tree species such as baobabs.

2.4 Crossdating and chronology building

The austral growing season spans two calendar years. For dating purposes, each tree ring was assigned to the year in which the growth started (following Schulman 1956). The resulting tree-ring width time series were synchronized with TSAPWin (Time Series Analysis and Presentation for Dendrochronology and Related Applications; version 4.67c © 2002–2011 Rinntech). The program allows visual and statistical crossdating by matching patterns of thin and wide rings (Fritts 1976) and illustrates discrepancies between the series. Areas of uncertain dating were reviewed in WinDENDRO™ and corrected if necessary. The program Cofecha (Version 6.06P © 1997–2004 Absoft Corporation) was used to detect possible measurement errors and to verify the crossdating. Owing to difficulties during the crossdating process each tree-ring width time series was plotted against the annual precipitation amount as a function of time. By comparing ring-width and precipitation data, annual growth patterns could be recognized. Ring-growth and precipitation curves were synchronised by adding missing rings or deleting false rings. As few changes as possible were applied following the principle of parsimony (Fig. 3a, b).

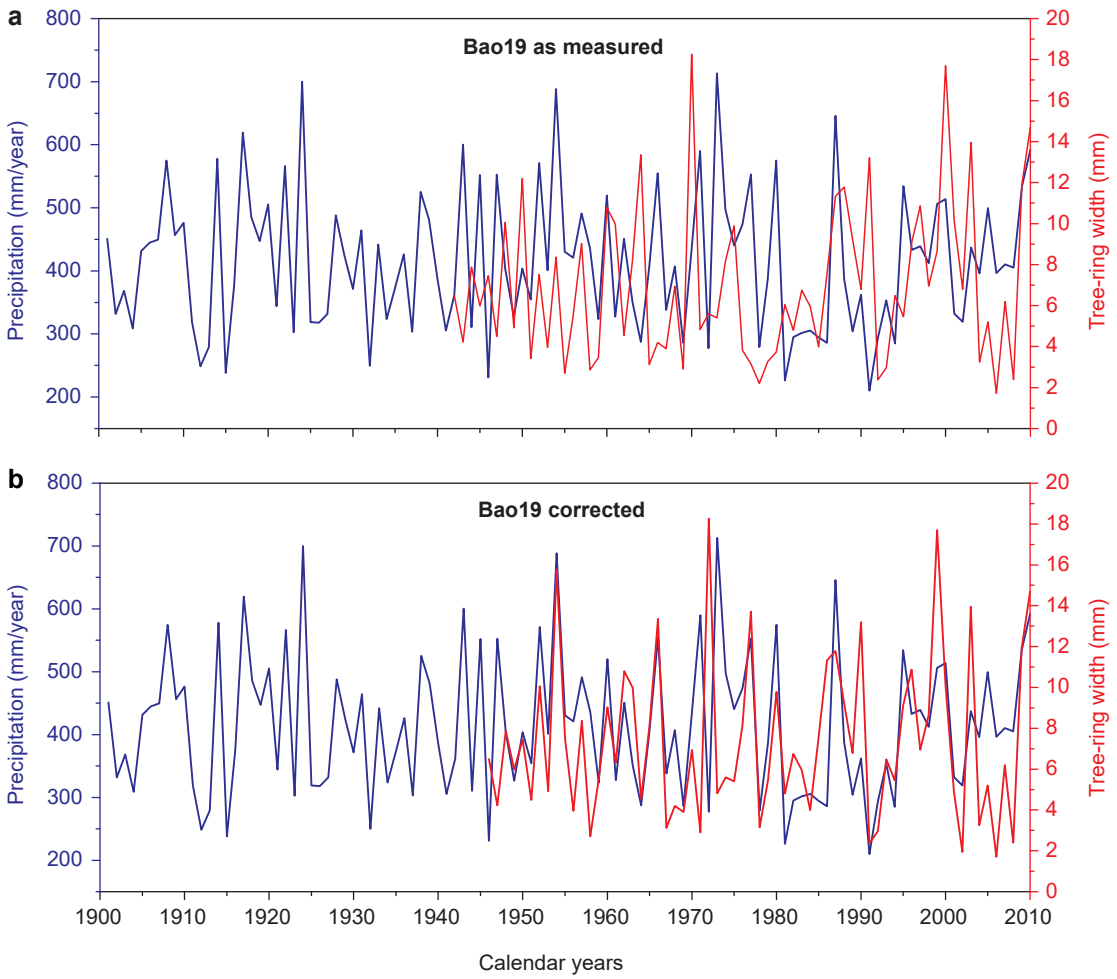

Fig. 3: Comparison between (a) measured and (b) corrected tree-ring width time series plotted against the annual precipitation amount adjusted for the austral growing season (*CRU TS3.10.01*). Following the principle of parsimony, the least possible changes were applied (*here: 6*) to synchronize the TRW measurement with the annual precipitation amount. Thus, it was abstained from fitting all major peaks together (*see: 1972/1973*) since one correction would have caused two additional changes. Omitting the corresponding TRW value for 1970 in (a) and 1972 in (b) the rank order correlation was improved from $rho_a = 0.10$, $p_a = 0.43$ to $rho_b = 0.46$, $p_b < 0.001$.

The program ARSTAN (AutoRegressive STANdardization; MRWE Application Framework © 1997–2004 Absoft Corporation) was used to produce a baobab tree-ring width (TRW) chronology from the individual time series. Measured series were detrended and indexed before a robust estimation of the mean value function was applied to remove effects of endogenous stand disturbances (Cook and Holmes 1986). Adaptive power transformation (Cook and Peters 1997) was chosen to stabilise the variance of the ring-width series. Age related growth trends, caused by fast juvenile and slow adult growth, were eliminated with Hugershoff growth curve, i.e. a combination between polynomial and exponential functions. They optimally compensate the values of the tree-ring widths produced at different age stages (Schweingruber 1983).

2.5 Stable isotope analyses

To verify the sample dating and to gain more information about the species' climate response, stable carbon ($\delta^{13}C$) and oxygen ($\delta^{18}O$) isotope values were analysed for the 20 outermost rings of 16 and 4 baobab trees, respectively. Tree rings were cut with a scalpel, by separating the diffuse porous wood (X) from the terminal parenchyma band (TB; i.e. two samples per year). Tree rings that include false rings were split for checking purposes. The samples were dried overnight in a vacuum drying chamber at 40 °C. Cellulose was extracted after Wieloch et al. (2011) and homogenized by ultrasonic treatment (Laumer et al. 2009). After drying in a vacuum freeze dryer for at least 48 h, 180–220 µg (170–200 µg) cel-

lulose samples as well as reference material were packed in tin (silver) capsules for $\delta^{13}C$ ($\delta^{18}O$) analysis. Measurements of stable carbon isotopes were carried out by combustion (1080 °C), using an elemental analyser (Model NA 1500; Carlo Erba, Milan, Italy) coupled online via an open split to an Isoprime IRMS (Isoprime Ltd, Cheadle Hulme, UK). Samples for $\delta^{18}O$ analysis were stored in a dry chamber before measurements were performed by high temperature TC/EA pyrolysis (1400 °C) coupled online via a Conflo IV to an IRMS Delta V Advantage (Thermo Fisher Scientific, Bremen, Germany). Helium 5.0 was used as carrier gas for all analyses. The reproducibility of sample (reference) material measurements was better than ± 0.1 ‰ (± 0.1 ‰) for $\delta^{13}C$ and ± 0.2 ‰ (± 0.3 ‰) for $\delta^{18}O$, respectively. The isotope ratios are given in delta (δ) notation, relative to VPDB (for $\delta^{13}C$) or VSMOW (for $\delta^{18}O$) as standard material (Craig 1957).

2.6 Correlation with climate quantities

Data of the isotopic composition of precipitation in and around southern Africa provided by the IAEA (International Atomic Energy Agency) was used for comparison with the obtained mean $\delta^{18}O$ time series of X, TB and Mix (=(X+TB)/2). The carbon isotope discrimination ($\Delta^{13}C$) that occurs during photosynthetic CO_2 uptake of C_3 plants was calculated after Saurer et al. (2004) by removing the atmospheric trend from the measured $\delta^{13}C$ values. Hence, the discrimination values reflect the plant response to weather conditions and changes in atmospheric CO_2 concentration.

All chronologies (TRW, $\Delta^{13}C_{X,\ TB,\ Mix}$, $\delta^{18}O_{X,\ TB,\ Mix}$) were correlated with monthly data of precipitation, cloud cover, temperature, and vapour pressure (CRU TS3.22), surface solar radiation (SSI; FRESCO v06), and Palmer Drought Severity Index (PDSI; PDSI.3.21.Penman.Snow.nl) for the grid field 19–23° S/24–28° E, as well as relative humidity anomalies (HADCRUH) for the grid field 20–25° S/25–30° E. The correlations cover a 24-month period and also include quarterly and annually resolved values for the austral growing season (i.e. July–June). It might seem questionable to correlate a precipitation based tree-ring width chronology with precipitation again, but in doing so information about the influence of individual months on wood growth can be obtained. The correlation values gained provide estimates about positive or negative effects of seasonal weather conditions on tree growth.

2.7 Calculation of intrinsic water-use efficiency (iWUE)

In plants, carbon uptake from the atmosphere and water loss are inherently linked, as both are controlled by stomatal movements (Farquhar and Sharkey 1982). The ratio of net photosynthesis (A) to conductance for water vapour (g_{H_2O}) on leaf-level is defined as intrinsic water-use efficiency (iWUE) that can be calculated from ^{13}C discrimination and atmospheric CO_2 concentration (pCO_2; for further information see e.g. Farquhar et al. 1982; Seibt et al. 2008). To examine potential changes in iWUE over time, changes in the ratio of leaf internal CO_2 (c_i) and atmospheric CO_2 (c_a) partial pressure of each tree (dc_i/dc_a) were used to define the plant response to recent pCO_2 increase as passive ($dc_i/dc_a = 1$), active ($dc_i/dc_a = c_i/c_a$), or very active ($dc_i/dc_a = 0$) according to Wang and Feng (2012).

3 Results

3.1 Comparative methodology for visual analysis of baobab wood anatomy

The preserved core samples showed alternating lighter and darker areas visible to the naked eye (Fig. 4a). Observation through a reflected light microscope exposed the lighter areas as diffuse porous wood (X) ranged by darker concentric parenchyma bands (TBs). Some samples showed considerable proportions of bark (up to 15 cm). Using reflected light, not all tree-ring boundaries could be identified with certainty, especially after remoistening the cores with purified water to prevent drying and irregular shrinking. Transmitted light yielded better results, but involved a greater sample material loss, due to the preparation of thin cross sections. UV light was found to be the best to identify baobab wood anatomical features (Fig. 4b–f). Fibres and parenchyma appeared in clearly distinguishable fluorescence colours. Due to their lignification, fibre cells and vessels appeared blue, whereas parenchyma cells showed colours from turquoise blue to violet pink. Thus, even very thin parenchyma bands could be detected and parenchyma enriched areas differentiated from true terminal parenchyma bands. Moreover, some parenchyma cells located next to fibres were found lignified. The width of terminal parenchyma bands varied greatly and seemed to be independent from the proportion of the preceding diffuse porous wood.

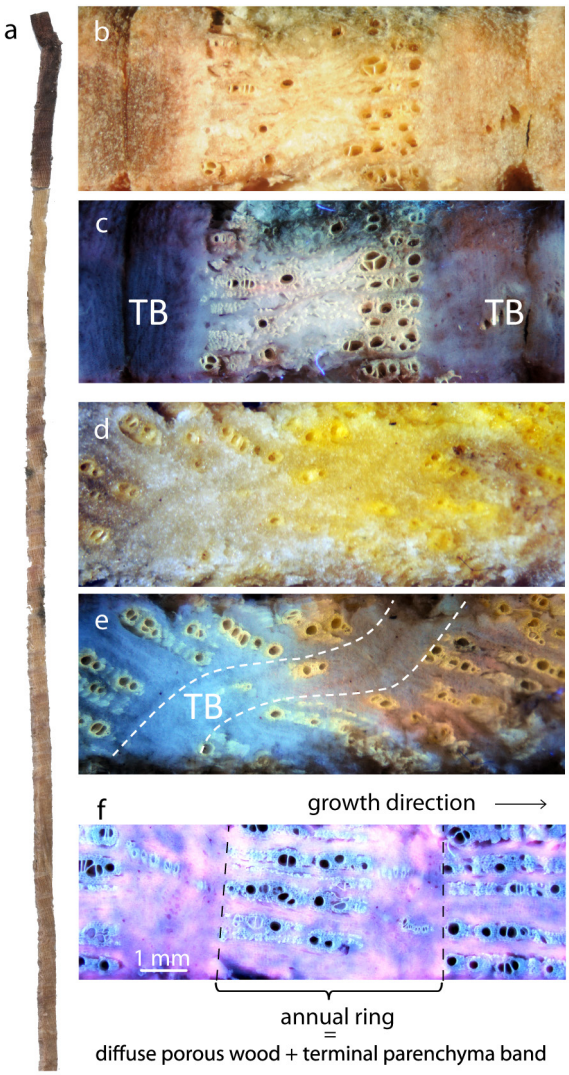

Fig. 4: Surface cut baobab core sample. (a) Overview image of a 5 mm thick baobab core sample with bark on top. Alternating lighter and darker areas indicate tree rings. Blackish discolouration is caused by partial mould formation. (b-e) Comparison of problematic areas using reflected and UV light (image height about 5 mm). (b) Uncertain wood anatomy between two terminal parenchyma bands (*TB*) can be recognized as parenchyma enriched area without vessels (c). (d) Confusing, parenchyma dominated area appears as a diagonally running terminal parenchyma band (e). (f) Image of a baobab tree ring under UV light.

Comparative measurements on moist and dried cores in WinDENDRO™ revealed similar but not identical results in number and width of tree-rings (Fig. 5). Parenchyma tissue shrinks much more than fibres and vessels, so that tree-rings with high parenchyma content shrank stronger than those with less parenchyma tissue. After drying, several very thin terminal parenchyma bands were no longer detectable. Furthermore, parenchyma rich areas were misinterpreted as TBs after drying. Where drying related split-offs were not associated with a thick TB, it was hard to interpret the wood anatomy next to the splits.

3.2 Special features of terminal parenchyma bands (TBs)

The comparison of two samples from the same tree revealed varying thicknesses of TBs for different radii of the stem. For some core samples the TBs close to the bark were only a few cells wide and difficult to distinguish from other radially orientated parenchymal bands that occasionally occured throughout the wood. Few TBs were shifted along woody rays (Fig. 6a), as commonly known for ring porous oak species. TBs can contain single vessels (Fig. 6b) or a row of vessels, i.e. a thin diffuse porous xylem section between two TBs (Fig. 6c–d). The alternation between diffuse porous xylem and parenchyma may not only reflect an annual growth rhythm, but may be also interpreted as short-term changes of growth conditions; presumably at the beginning or the end of a vegetation period. Other TBs were transversely interrupted by vessels and fibres, with a deviation of the enclosed woody rays from the outer rays (Fig. 6e–f). Individual triangle shaped transitions from woody rays to TBs occurred in 5 out of 20 samples (Fig. 6g). Some wedging rings could be identified (Fig. 6h). Consequently, missing rings have also to be considered. A few TBs tapered greatly and apparently vanished (Fig. 6i). A square shaped radial vascular bundle within a TB was detected only in 1 out of 20 samples (Fig. 6j). However, open vascular bundles were very common in all kind of parenchymal tissue, independent of its age. These usually collateral, seldomly bicollateral vascular bundles were orientated in a radial, tangential or horizontal axis (Fig. 6k–l). Phloem and xylem tissue occurred at either side of a fascicular cambium. Vascular bundles in TBs often showed dark lines extending the fascicular cambium at both sides. These thin cell rows may connect neighboured vascular bundles along a TB. Whilst drying and shrinking, core samples commonly split off along these cell lines.

3.3 Population's homogeneity

Analyses of long-term trends allowed for conclusions on the development of tree-ring proxies over time, without requiring secured ring counting and absolutely correct dendrochronological dat-

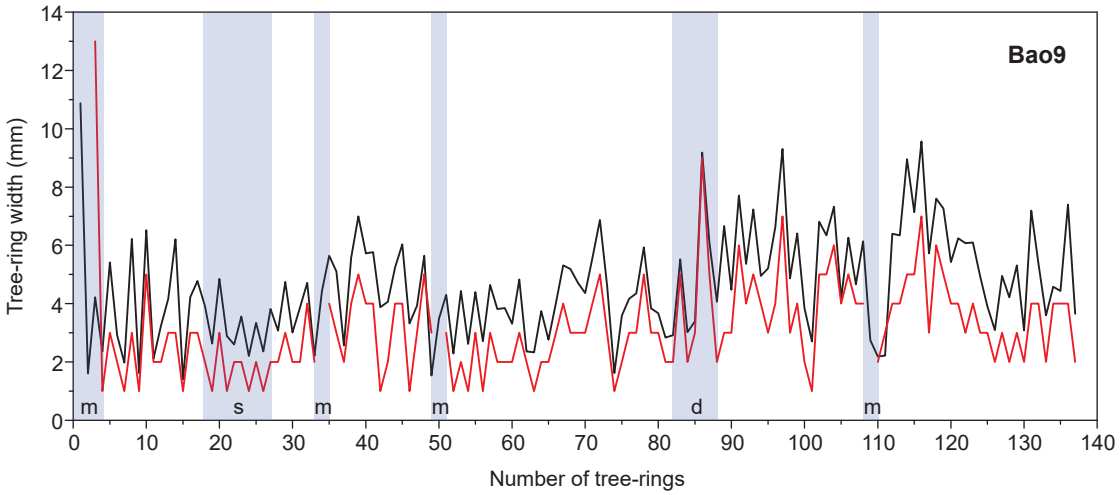

Fig. 5: Comparative measurement results for Bao9 wet (*black*) and dry (*red*). Some very thin terminal parenchyma bands could no longer be identified on the dried sample, thus causing missing rings (*m*). Partial areas shrank substantially, retaining similar proportions (*s*) whereas others shrank disproportionately (*d*). The original tree-ring width relations were generally altered during the drying related material shrinking.

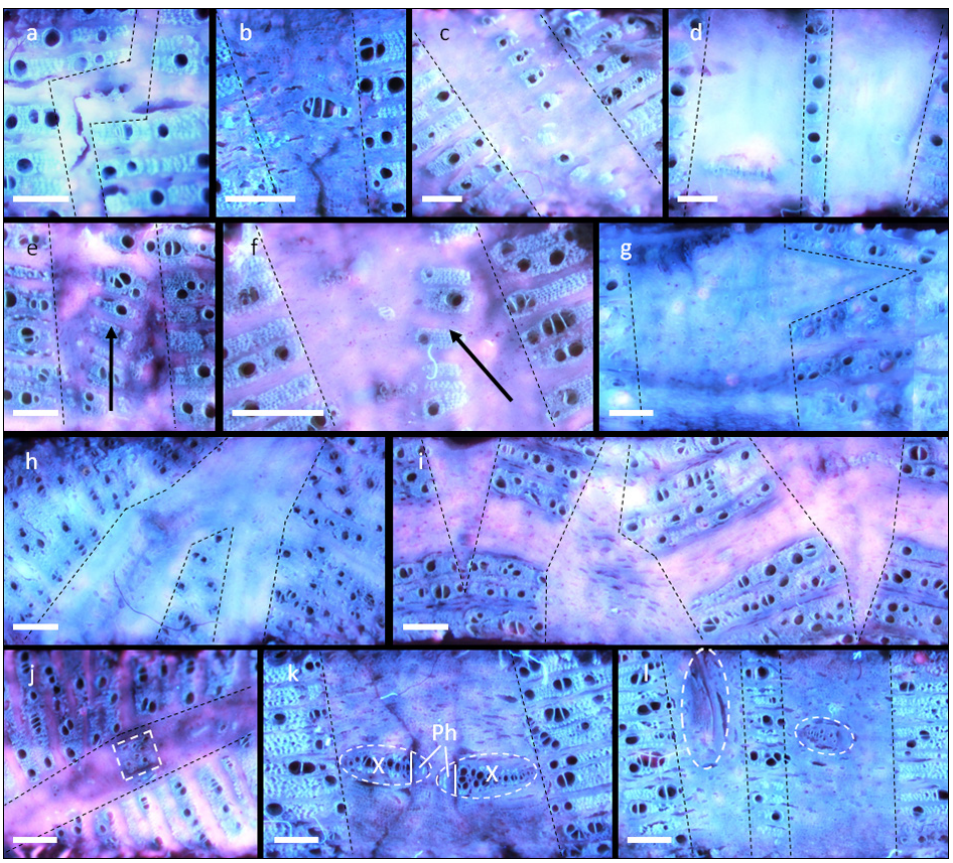

Fig. 6: Special features of terminal parenchyma bands (TBs; framed by black dotted lines) under UV light (white scale equals 1 mm). (a) TB got shifted along a woody ray. (b-d) Vessels enclosed in TBs: (b) Solitary enclosed vessel. (c-f) TBs split by vessels and fibres: (c-d) Single row of vessels and fibres splits TB. (e-f) Transversely by vessels and fibres interrupted TB shows enclosed woody rays deviating from outer rays. (g) Triangle shaped transition from woody ray to TB. (h) Merging ring. (i) Greatly tapering TBs seem to vanish. (j) Square shaped radial vascular bundle. (k-l) Collateral vascular bundles within TBs: (k) Two opposing collateral vascular bundles with xylem (*X*), phloem (*Ph*), fascicular cambium (*white lines*), and dark cell rows extending the fascicular cambium to either side of the bundle. (l) Two collateral vascular bundles either radially (*left*) or horizontally (*right*) orientated.

ing. Due to wood anatomical characteristics, the 2009/2010 tree-ring boundary could not be identified with certainty in 7 out of 16 trees; thus, the 2010 tree ring was defined as missing for those samples. To ensure comparability among the studies, all further statements refer to the period 1991 to 2009.

The mean annual growth of baobabs on Kubu Island amounted to 6.02 mm (minimum 2.42 mm for Bao9, maximum 11.55 mm for Bao20; table 2) with a mean variance of 10.76 mm. The variance increased significantly with rising growth rates ($r = 0.86$, $p < 0.001$; Fig. 7a). The individual growth over time showed no common trend with 9 trees slightly increasing (Bao20 significantly with $p < 0.05$) and 7 trees slightly decreasing in their growth per annum. No significant relationship could be found between stem circumference and growth trends.

The grand mean $\delta^{13}C$ ($\delta^{18}O$) values of -26.24 ± 0.91 ‰ VPDB (29.81 ± 1.19 ‰ VSMOW) were found with higher individual tree mean $\delta^{13}C$ ($\delta^{18}O$) values showing significantly lower (higher) variances ($r_{\delta 13C} = 0.54$, $p < 0.05$; Fig. 7b; $r_{\delta 18O} = 0.98$, $p < 0.05$; Fig. 7c; Tab. 2). Regarding the ^{13}C discrimination, significant negative trends (5 trees) dominated significant positive trends (2 trees) over time ($p < 0.05$). No significant relationship could be found between the values for discrimination, growth rates or $\delta^{18}O$, respectively. Concerning changes in iWUE, 10 trees responded actively or very actively to the elevated atmospheric CO_2 content, 5 of them significantly ($p < 0.05$–0.0001), with $0 < dc_i/dc_a < c_i/c_a$. Four baobab trees responded less actively, 3 of them significantly ($p < 0.01$–0.0001), with $c_i/c_a < dc_i/dc_a < 1$, and the remaining 2 trees responded passively ($p < 0.001$–0.0001) with $dc_i/dc_a \geq 1$. Therefore, iWUE increased in 14 out of 16 baobab trees in a range of 2.2–30.7 %.

3.4 Verification of the preliminary chronology and population's climate response

Of the 1197 tree rings that were measured on 20 core samples, 101 corrections have been applied (74 false rings, 27 missing rings), which results in an error rate of 8.4 %. Missing rings include also the counts for 2010 and were omitted from the analysis. The preliminary TRW chronology for the 16 baobab trees covering the period 1960–2009 is given in Fig. 8a, b. The stable isotope data failed to prove the sample dating, because the obtained $\Delta^{13}C$ and $\delta^{18}O$ time series could not be crossdated among different trees (Fig. 9). The splitting of suggested multiple rings into tree rings could not increase the correlation coefficient.

TRW correlated significantly with the rainfall amount of the peak wet season, January–March (JFM), especially with February (JFM: $r = 0.67$, $p < 0.001$; Feb: $r = 0.66$, $p < 0.001$) and significantly with previous September (sep: $r = 0.29$, $p < 0.05$; Fig. 10a). A very similar pattern was observed for cloud cover (JFM: $r = 0.58$, $p < 0.001$; Feb: $r = 0.66$, $p < 0.001$; sep: $r = 0.38$, $p < 0.01$; not shown). During the peak wet season the chronology showed a significant negative correlation with temperature (JFM: $r = -0.40$, $p < 0.01$; February: $r = -0.44$, $p < 0.01$; Fig. 10b). No significant correlations were observed between tree-ring width and vapour pressure, relative humidity anomalies or SSI (not shown). Significant positive correlations were achieved between TRW and PDSI from January to September with highest values in February ($0.37 \leq r \leq 0.54$; $p < 0.01$; not shown).

Although $\Delta^{13}C$ and $\delta^{18}O$ could not be crossdated among different trees, mean values were correlated with climate data, in case an underlying climate signal is superimposed by individually controlled reactions to e.g. site conditions.

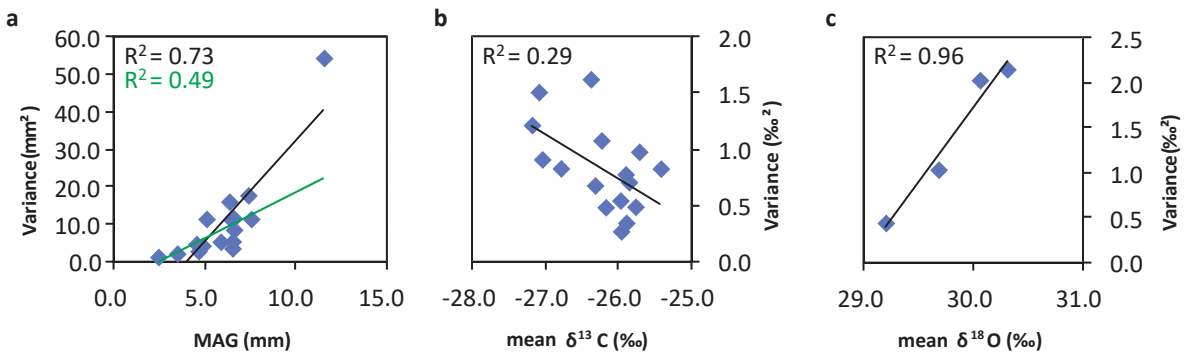

Fig. 7: Variance analyses. (a) mean annual growth (*MAG*; *black*: r = 0.86, p < 0.001); without outliner (*green*): r = 0.70, p < 0.01). (b) $\delta^{13}C$ (r = 0.54, p < 0.05). (c) $\delta^{18}O$ (r = 0.98, p < 0.05).

Tab. 2: Mean, minimum, maximum and variance values of TRW, $\delta^{13}C$, and $\delta^{18}O$ for the period 1991–2009

Tree	annual growth (mm)				$\delta^{13}C$ (‰ VPDB)				$\delta^{18}O$ (‰ VSMOW)			
	mean	min	max	variance	mean	min	max	variance	mean	min	max	variance
Bao1	6.50	3.30	11.77	3.57	-26.80	-28.53	-25.14	0.83				
Bao3	6.47	1.49	15.58	11.16	-25.91	-29.19	-24.70	0.78				
Bao4	5.86	1.94	10.58	5.33	-25.97	-26.94	-24.86	0.27				
Bao6	6.59	1.39	13.44	8.56	-25.77	-27.01	-24.60	0.49	29.18	27.87	30.92	0.47
Bao9	2.42	0.85	5.01	1.28	-25.72	-27.59	-23.98	0.98				
Bao10	6.57	2.11	15.55	11.63	-25.86	-27.75	-23.56	0.71	30.04	26.34	32.08	2.17
Bao11	4.86	1.11	10.82	4.31	-27.05	-28.61	-24.83	0.91	30.33	27.58	35.27	2.26
Bao14	6.33	1.26	16.89	16.06	-25.42	-26.95	-23.46	0.83				
Bao15	6.51	2.74	11.47	5.44	-27.10	-29.62	-25.16	1.51				
Bao17	3.46	1.37	7.31	2.17	-26.39	-28.62	-23.77	1.63				
Bao19	7.38	1.71	17.70	17.78	-27.20	-28.80	-25.36	1.22				
Bao20	11.55	3.12	37.52	54.48	-26.24	-28.09	-24.66	1.08				
Bao21	4.64	1.36	7.65	2.85	-26.33	-27.61	-24.64	0.68				
Bao22	4.52	1.89	9.16	4.73	-25.90	-26.95	-24.51	0.35	29.65	27.36	31.77	1.04
Bao23	7.54	3.46	14.19	11.43	-26.18	-27.92	-24.94	0.49				
Bao24	5.07	1.61	15.69	11.44	-25.98	-27.24	-24.97	0.55				

Most of the mean $\Delta^{13}C$ and $\delta^{18}O$ time series correlated significantly with the pre-selected climate parameters ($p < 0.05$) and correlations were scattered throughout the year. $\Delta^{13}C_X$ correlated overall negatively with relative humidity anomalies (Fig. 10c), whereby significant values were reached for the previous quarters July–September (jas: $r = -0.59$, $p < 0.05$) and October–December (ond: $r = -0.68$, $p < 0.05$) with highest values for July (jul: $r = -0.62$, $p < 0.05$) and December (dec: $r = -0.79$, $p < 0.01$), respectively. Further significant correlations were found for September/October (Sep: $r = -0.58$, $p < 0.05$; Oct: $r = -0.64$, $p < 0.05$), and the annual mean ($r = -0.59$, $p < 0.05$).

Correlations with PDSI were negative and generally highly significant for $\Delta^{13}C_{Mix}$ and negative and generally significant for $\Delta^{13}C_X$ throughout the year, except for January/February or previous November to February, respectively.

From the available GNIP station data sets Harare and Pretoria showed highest correlations with the monthly precipitation amount ($r_{Harare} = -0.93$, $p < 0.0001$; $r_{Pretoria} = -0.82$, $p < 0.0001$) as well as temperature around Kubu Island ($r_{Harare} = -0.63$, $p < 0.05$; $r_{Pretoria} = -0.76$, $p < 0.01$). Unfortunately, the data coverage for both stations is very scarce during 1991–2009. There were only 2 years available for Harare (1999, 2001) and 5 years for Pretoria (1996–2000) with at least 7 months of data to be averaged. No significant correlation was found for $\delta^{18}O_X$, $\delta^{18}O_{TB}$ or $\delta^{18}O_{Mix}$ with $\delta^{18}O_{Pretoria}$. Nevertheless, $\delta^{18}O_X$ and $\delta^{18}O_{Mix}$ were positively correlated with the rainfall amount of the previous quarter October–December (ond: $r_X = 0.55$, $p < 0.05$; $r_{Mix} = 0.52$, $p < 0.05$; Fig. 10d) with $\delta^{18}O_{Mix}$ being correlated with previous November as well (n: $r_{Mix} = 0.51$, $p < 0.05$) and $\delta^{18}O_X$ showing negatively correlations with the rainfall amount of the following November (Nov: $r = -0.47$, $p < 0.05$). The shift from slightly positive to slightly negative correlations of $\delta^{18}O_X$ and $\delta^{18}O_{Mix}$ with precipitation amount is in line with the annual course of $\delta^{18}O_{Harare}$. The same shift is visible for correlations with temperature, although far from being significant (not shown).

4 Discussion

Working on baobab trees involves practical challenges in sample preservation, preparation, data collection, and data assessment. Airtight packing, cool storage and quickest possible freezing of

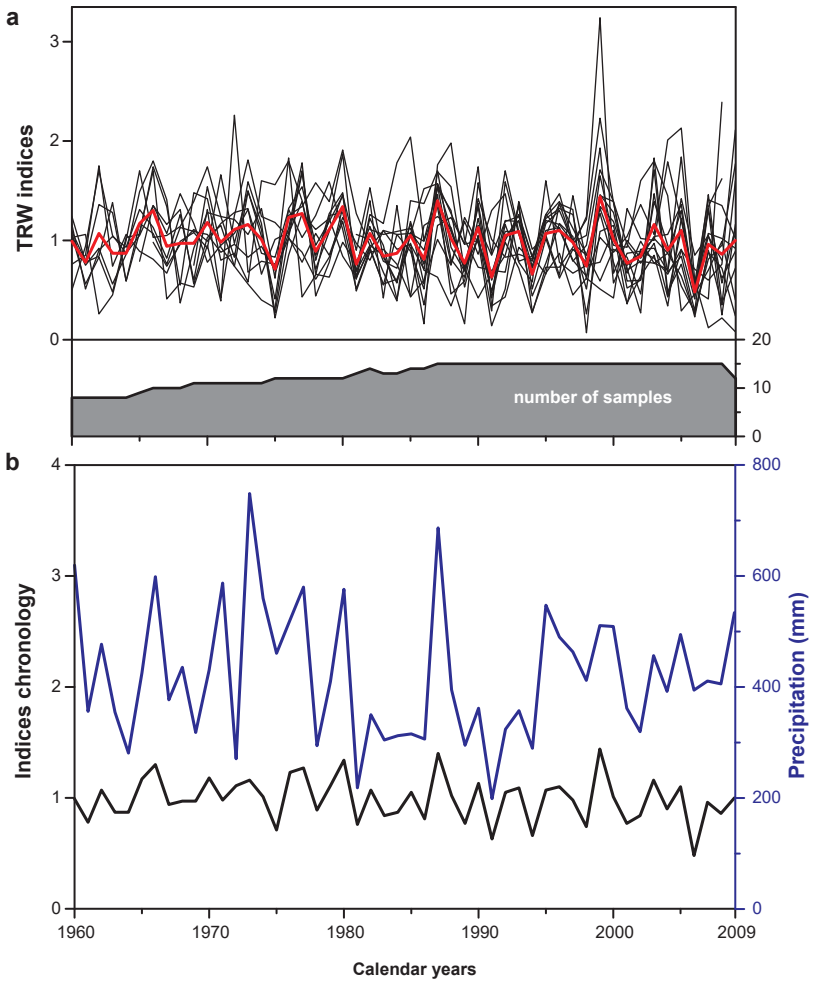

Fig. 8: Preliminary baobab chronology. (a) Visual crossdating of 16 core samples with resulting TRW indices chronology (red). Missing rings were treated as gaps in the series. (b) Comparison of the TRW indices chronology with annual precipitation data corrected for the austral growing season (*CRU TS3.10.01*).

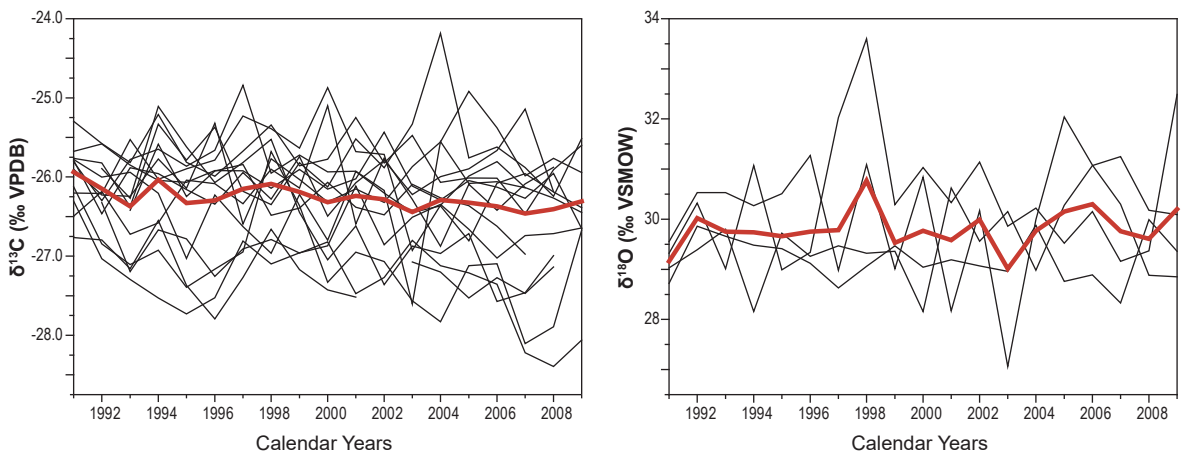

Fig. 9: $\delta^{13}C$ and $\delta^{18}O$ values for 16 and 4 samples, respectively, with the mean values in red. Assumed false rings were temporary treated as tree rings for test purposes, but the correlation coefficient could not be increased that way.

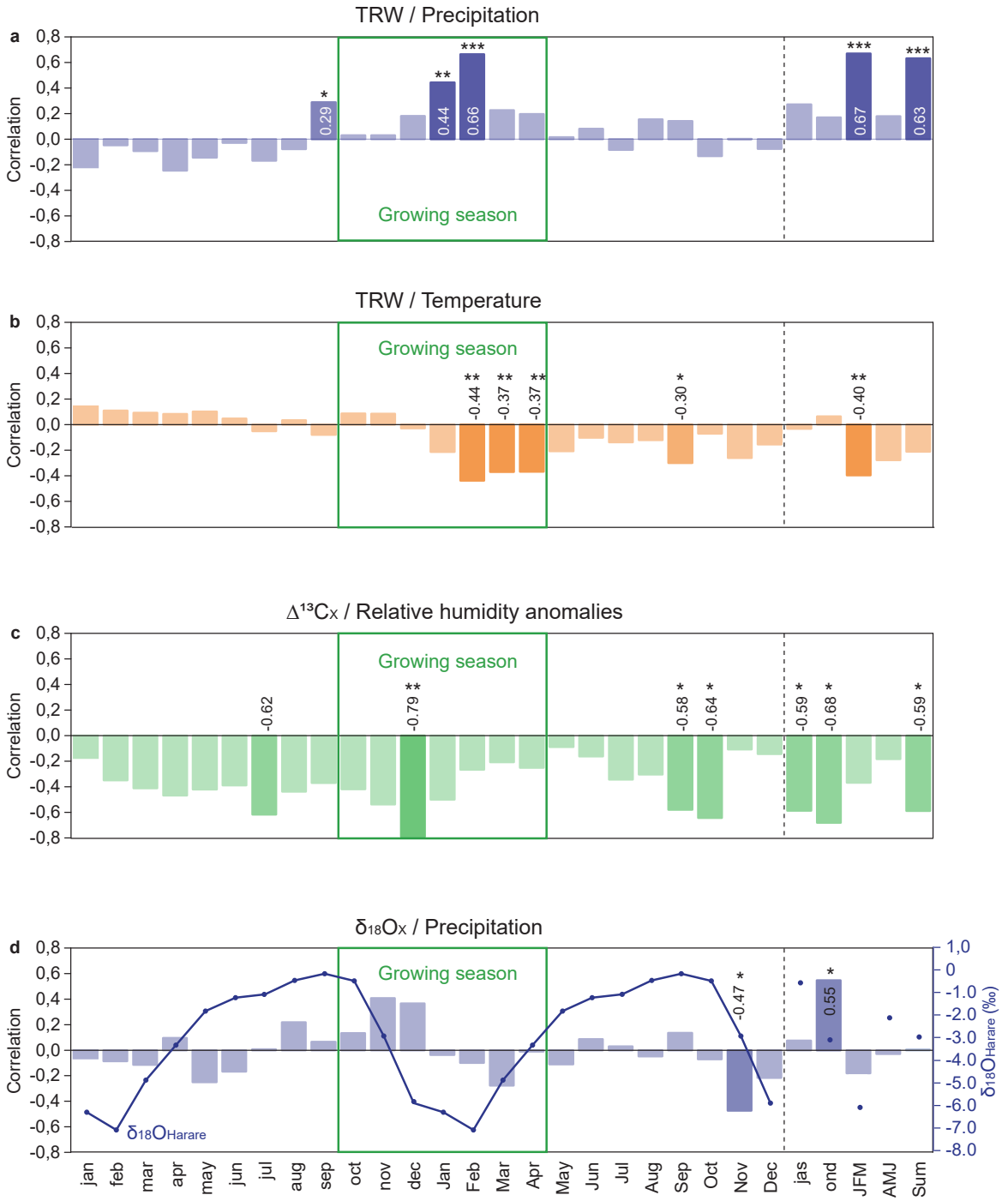

Figure 10: Correlations between TRW, Δ¹³C, and δ¹⁸O with climate indices (*CRU TS3.22: 19-23°S, 24-28°E; * p < 0.05, ** p < 0.01, *** p < 0.001*). Months of the austral growing season's first year start with small letters, months of the second year with capital letters. (a) TRW correlates highly significant with the annual precipitation amount (*Sum*), especially during the peak wet season (*JFM*) with highest values in February. (b) TRW correlates highly negative with the temperature during the peak wet season (*JFM*) as well as in April with highest values in February. (c) Discrimination values are overall negatively correlated with relative humidity anomalies (*HadCRUH: 20-25°S, 25-30°E*): significantly for the annual mean, as well as previous July and September/October. Highest values are archived for previous December. (d) Positive correlations of $\delta^{18}O_x$ values with the previous season from October to December (*ond*) switch to increasing negatively correlations from January to March (JFM). This stepwise change during the growing season is in line with the seasonal course of the δ¹⁸O values for precipitation from Harare (*blue line*). Significant negative correlations are found for November.

the samples could not completely prevent mould formation. Fungus development was most commonly indicated by very few, small scattered areas of surface discolouration or even fewer discolouration throughout the core, without any effect on the wood texture. Comparative measurements have shown that air drying of baobab wood samples leads to major information losses: very thin parenchyma bands could become undetectable, parenchyma rich areas were likely to be misinterpreted as terminal parenchyma bands, and the relation between individual tree-ring widths was altered due to the drying related material shrinking. More gentle drying processes like drying over several weeks (Robertson et al. 2006) or freeze-drying may offer alternatives for working with moist core samples and may be tested further in future studies.

UV light induced fluorescence was found to be best suited for the identification of baobabs' wood anatomical details. Nevertheless, their interpretation remains challenging in many cases. The characteristic features of terminal parenchyma bands cover a wide range (Fig. 6). The identification of tree-ring boundaries was complicated by disproportionately thin parenchyma bands, as well as multiple, wedging, greatly tapering and apparently vanishing rings. The occurrence of vessels in terminal parenchyma bands was not unusual. Adjacent bands separated only by a row of vessels could either describe a short intra-seasonal rainfall event during the dry season, or the termination of two individual vegetation periods. A noticeable number of vascular bundles appeared in all kinds of parenchymal tissue. One sample showed a square shaped radial vascular bundle within a terminal parenchyma band, which is rather typical for roots than for trunks (Denffer 1983). Most of the vascular bundles, however, are open collateral bundles without a specific orientation. Since they were always embedded in parenchymal tissue, they may have caused the observed triangle shaped transitions from woody rays to terminal parenchyma bands. Intraxylary vascular bundles in baobabs have been described earlier by Fisher (1981) and Rajput (2004) and were associated with the regeneration of damaged tissues. Caused by external injuries or probably age-related internal damages, adjacent parenchyma cells start to proliferate (Fisher 1981) and can form meristematic centres, which differentiate on repeated divisions into vascular bundles (Rajput 2004). Because Rajput (2004) found these structures solely in xylem produced 12–15 years ago, he assumed it to be an age-related phenomenon. However, core samples from Kubu Island showed vascular bundles age-independently in all kind of parenchymal tissue, which contradicts the hypothesis of an age-related phenomenon.

Following the Hagen-Poiseuille equation, the capillary fluid flow rate for a given pressure gradient depends on the fourth power of vessel radius. Furthermore, longer vessels show a larger conductivity due to a decreased passage of fluids from cell to cell (Roth-Nebelsick 2006). That results in a decreased transport resistance within a vascular strand. The frequent occurrence of vascular bundles throughout the wood of baobab trees is thus likely another adaption to the semi-arid environment, enabling greater water storage and a more effective nutrient transport.

Apart from the challenging wood anatomy, site and age differences were likely responsible for the encountered difficulties in crossdating the tree-ring width series. To sample all available age classes turned out to be problematic, since baobabs of several age classes show different growth rates (Swart 1963; Guy 1970; Guy 1982; Breitenbach 1985) and react quite individually to poor, inconsistent or heavy rainfall. Two neighbouring baobab trees growing under the same site conditions were found to show strongly different growth trends over the last 19 years; most likely due to age differences expressed by circumference (Bao20: 2.5 m, Bao21: 5.5 m). While the thicker tree grew constantly slow, the other one showed an exceptional growth increase over time. All other observed growth trends seemed to be independent from the individual stem circumference and were thus very likely due to site differences. A tree located at a slightly inclined and weakly fissured granite rock showed constantly below average growth rates (Bao9), because the absence of soil resulted in a lack of nutrients and water. Beside these exceptions (Bao9, Bao20), all sampled trees showed similar mean values for annual growth.

Mean $\delta^{13}C$ values varied about 1.8 per mille between trees, which is relatively little compared to 3 or up to 5 per mille stated for trees in other studies (Loader et al. 2003; Skomarkova et al. 2006; Gebrekirstos et al. 2011). An increase in mean $\delta^{13}C$ values was accompanied by decreasing variances most likely due to plant-physiological processes. High $\delta^{13}C$ values can be governed by very low stomatal conductance (i.e. drought stress) and/or a very high rate of photosynthesis (unlikely under drought stress). Both lead to a drop in the leaf internal CO_2 concentration, whereby the photosynthetic

enzyme RubisCO discriminates less against ^{13}C (e.g. Scheidegger et al. 2000; Mccarroll and Loader 2004; Treydte et al. 2004). As stress ceases, the ratio of photosynthetic rate and stomatal conductance can be increasingly influenced by factors as site and age differences, which cause higher $\delta^{13}C$ variability. These influences might also be responsible for the missing relationship between discrimination and growth rates.

The rising CO_2 concentration of the atmosphere (c_a) and the related decreasing $\delta^{13}C$ value, primarily due to the combustion of isotopically light fossil fuels over the last 200 years, are likely to trigger plant physiological responses. Wang and Feng (2012) found the increase in c_a accounting for 98 % of the observed changes in iWUE of 83 tree-ring $\delta^{13}C$ series from northern hemisphere mid- to high-latitudes. It seems thus by far being the most important variable in driving the iWUE changes over time. As c_a increases, more or increasing amounts of CO_2 will diffuse into the leaves. Because c_i was found to increase linearly with c_a, the increasing CO_2 transfer into the leaves has been greater than the rate of CO_2 fixation. Due to plant physiological adaptations c_i increased less rapidly than c_a so that $dc_i/dc_a < 1$, which causes iWUE to increase (Wang and Feng 2012). The majority of baobab trees responded actively to the elevated atmospheric CO_2 content. This could be either by increasing their photosynthetic rate and/or by decreasing stomatal conductance. Since water availability is the main limiting factor in arid regions, the latter seems to be more appropriate. The increasing trend in iWUE has already been shown for other tree species at different locations worldwide (Duquesnay et al. 1998; Saurer et al. 2004; Brienen et al. 2010). However, it is interesting to note that an increase in iWUE does not necessarily lead to an overall reduction in transpiration as demonstrated in a recent study by Frank et al. (2015). In fact their models calculated a 5 % increase in European forest transpiration over the 20th century. Hence, other factors such as enhanced leaf-area index, prolonged growing season, and increased evaporative demand (Frank et al. 2015) seem to counteract theoretically mitigating effects of increased iWUE.

Mean $\delta^{18}O$ values varied about 1.1 per mille, which is in the lower range of other studies (Norström et al. 2008; Sano et al. 2012; Schollaen et al. 2014). In contrast to $\delta^{13}C$, increasing $\delta^{18}O$ values were accompanied by increasing variances. Various exchange mechanisms between enriched water from the site of evaporation or subsequently built sugars and unenriched xylem water, transported via the transpiration stream, impede a straightforward interpretation of ^{18}O enrichment found in tree-ring cellulose (Gessler et al. 2014). A high rate of transpiration (due to wet and/or relatively cool environmental conditions) leads to an enrichment of leaf water, since isotopically lighter water evaporates faster. The so called Péclet effect causes the exponential nature of ^{18}O enrichment that reaches a maximum, when the enriched water is hindered to diffuse backwards in the leaf lamina by the opposing transpiration stream (Farquhar and Lloyd 1993; Barbour et al. 2001; Farquhar and Cernusak 2005; Treydte et al. 2014). Thus, enriched, mixed and xylem water are available for photosynthesis, and might have caused the higher variability of higher $\delta^{18}O$ values.

Low transpiration values, triggered by reduced stomatal conductance (due to dry and/or hot conditions), cause less evaporative enrichment of the leaf water. Hence, the difference in $\delta^{18}O$ of the leaf water and the reduced transpiration stream is less pronounced, which could explain the observed smaller variances for lower $\delta^{18}O$ values.

Baobab trees with higher mean $\delta^{13}C$ values showed smaller variances, probably because a higher stress level reduces the influence of individual differences in site and age conditions. At the same time baobabs with lower mean $\delta^{18}O$ values showed smaller variances, likely due to high vapour pressure differences between the atmosphere and the leaves, forcing the trees to behave more similar. The tree with the highest mean $\delta^{18}O$ had the lowest mean $\delta^{13}C$. That very young tree (Bao11) was part of a group of baobabs and seemed to be the least stressed tree of our sample collection. There was no significant correlation between high $\delta^{18}O$ values and low $\delta^{13}C$ values and vice versa, which could be due to the small sample size (4). Very little is known about the ecophysiology of baobabs and the range of variability. Therefore, our observations may only be an expression of individual morphometric differences between trees. Further studies are needed to clarify if the range of variation is meaningful in terms of stress versus non-stress situations or not.

Chronology building was based on the comparison of individual tree-ring width series and regional precipitation amount per annum. Since these two parameters were highly significantly correlated, missing and false rings could be identified. In consequence, the preliminary chronology needed to be confirmed by further analyses. Since the obtained $\Delta^{13}C$ and $\delta^{18}O$ time series could not

be crossdated among different trees, these analyses could not be used as a direct control of sample dating. However, the correlations and trends found between the stable isotope series and various climate parameters roughly met the model expectations for such an environment, suggesting common climate signals were superimposed by individual reactions to e.g. site conditions. Assuming that dendrochronological dating was correct, our results indicate that higher sample replication may be required for establishing appropriate stable isotope site chronologies. The fact that $\Delta^{13}C$ was found to correlate overall negatively with relative humidity anomalies and PDSI is in accordance with the Farquhar model, that low stomatal conductance leads to a decrease in c_i and thus an increase in $\delta^{13}C$ of plant material (Farquhar et al. 1982). This could prove the reliability of the sample dating. Contrary to our results, Robertson et al. (2006) found a positive correlation between detrended carbon isotope values for wholewood of a baobab specimen from Skukuza (24°59' S, 31°35' E), South Africa, with January precipitation. However, since their results are based on a single baobab growing close to a cultivated garden, where watering takes place if needed, their outcomes should be treated with caution. The highly significant negative correlations of the GNIP $\delta^{18}O$ data for Harare and Pretoria with precipitation amount and temperature is explained by the geographical site location. As situated in the summer rainfall zone both precipitation amount and temperature rise at the same time and the expected increase in $\delta^{18}O$ with temperature is superimposed by the rainfall amount effect. This trend holds true for the relation of baobab $\delta^{18}O$ to precipitation and temperature, expressed by the shift from positive to negative correlations during the growing season.

The significant correlations between tree-ring width indices and precipitation as well as cloud cover during the peak wet season (JFM) illustrate the high water demand of baobabs on Kubu Island during that period, mostly pronounced in February. A more dense cloud cover increases the probability of rain and decreases solar radiation, which is usually accompanied with high temperatures. These findings were confirmed by the concurrent negative correlation with temperature, whereas vapour pressure did not seem to influence baobab growth rates. Usually, it takes 2–3 months for baobabs to return to pre-flushing water-content levels in the stem (Chapotin et al. 2006c). As baobabs on Kubu Island showed highest correlation with the fourth month of the wet season (February), they apparently experienced a disproportionately high water loss during the dry season and thus needed more time for compensation. Nevertheless, the presented results should be treated with caution since possible dating errors in our preliminary chronology cannot be ruled out completely.

5 Conclusion

The African baobabs are promising yet challenging tree species for dendrochronological studies. While air tight packing and freeze storing ensures good sample preservation, and UV light induced fluorescence enables clear identification of wood anatomical details, interpreting the latter is still difficult. Site and age differences additionally increased the problems so that conventional crossdating failed. High-resolution ^{14}C analyses and subsequent ^{14}C wiggle matching might be an additional methodology to be applied for proper dating of baobab wood samples. However, the strong relationship between TRW and annual precipitation amount allowed the identification of missing and false rings and thus the development of a preliminary baobab chronology from 1960–2009. Despite TRW, $\Delta^{13}C$ and $\delta^{18}O$ were found to correlate significantly with climate data. Precipitation amount around Kubu Island showed highest correlations with the annual $\delta^{18}O$ course of precipitation from Harare. Due to the current data gaps in southern African GNIP stations, no correlations with the baobab $\delta^{18}O$ series could be applied. Hence, tree-ring verification using annually resolved $\delta^{18}O$ values of precipitation is not yet possible. Additional intra-annual stable isotope analyses might solve this problem, by allowing for correlations with the long-term $\delta^{18}O$ monthly mean values and should thus be applied in future studies. Other requirements for prospective dendrochronological studies on baobab trees include more comparable site conditions and the exclusion of obvious juvenile baobab trees from the sampling. We suggest a higher sampling rate with two or more samples per tree with larger core diameter (e.g. 12 mm) to overcome problems of apparently vanishing parenchyma bands. Although our results cannot unambiguously prove the correct sample dating, highly significant correlations and trends in line with established models of isotope fractionation indicate that baobab trees indeed show potential to become a new high-resolution climate archive for (semi-)arid Africa.

Acknowledgements

We appreciate the field assistance of Alexander Müller and thank Heiko Baschek, Carmen Bürger and David Göhring for their support in the laboratory. We are also grateful to Ingo Heinrich and Karina Schollän for fruitful discussions, to many helpful people in Botswana providing particular information, and to the Ministry of Minerals, Energy and Water Resources of Botswana for granting a research permit. Financial support was provided by the Deutsche Forschungsgesellschaft (DFG). Franziska Slotta received a predoctoral fellowship (Elsa-Neumann-Scholarship) of the federal state of Berlin.

References

Adanson, M. (1759): A Voyage to Senegal, the Isle of Goree, and the River Gambia. Translated from the French. With notes by an English gentleman who resided some time in that country. London.

Barbour, M. M.; Andrews, T. J. and Farquhar, G. D. (2001): Correlations between oxygen isotope ratios of wood constituents of *Quercus* and *Pinus* samples from around the world. In: Australian Journal of Plant Physiology 28, 335–348. https://doi.org/10.1071/Pp00083

Belingard, C.; Tessier, L.; Denamur, C. and Schwartz, D. (1996): Dendrochronological approach to the radial growth of okoume (Congo). In: Comptes Rendus De L Academie Des Sciences Serie Iii-Sciences De La Vie-Life Sciences 319, 523–527.

Breitenbach, F. V. (1985): Aantekening oor die groeitempo van aangeplante kremetartbome (*Adansonia digitata*) en opmerkinge ten opsigte van lewenstyd, groeifases en genetiese variasie van die spesie. In: Dendrologiese Tydskrif 5, 1–21.

Brienen, R. J. W.; Wanek, W. and Hietz, P. (2010): Stable carbon isotopes in tree rings indicate improved water use efficiency and drought responses of a tropical dry forest tree species. In: Trees 25, 103–113. https://doi.org/10.1007/s00468-010-0474-1

Chapotin, S. M.; Razanameharizaka, J. H. and Holbrook, N. M. (2006a): Baobab trees (*Adansonia*) in Madagascar use stored water to flush new leaves but not to support stomatal opening before the rainy season. In: New Phytologist 169, 549–559. https://doi.org/10.1111/j.1469-8137.2005.01618.x

– (2006b): A biochemical Perspective on the Role of large Stem Volume and high Water Content in Baobab Trees (*Adansonia* spp.; Bombacaceae). In: American Journal of Botany 93, 1251–1264. https://doi.org/10.3732/ajb.93.9.1251

– (2006c): Water relations of baobab trees (*Adansonia* spp. L.) during the rainy season: Does stem water buffer daily water deficits? In: Plant, Cell and Environment 29, 1021–1032. https://doi.org/10.1111/j.1365-3040.2005.01456.x

Cook, E. R. and Holmes, R. L. (1986): Program ARSTAN: Chronology development, statistical analysis. In Holmes, R. L.; Adams, R. K. and Fritts, H. C. (eds.): Tree-ring chronologies of western North America: California, eastern Oregon and northern Great Basin. Tucson, Az.

Cook, E. R. and Peters, K. (1997): Calculating unbiased tree-ring indices for the study of climatic and environmental change. In: The Holocene 7, 361–370. https://doi.org/10.1177/095968369700700314

Cooke, H. J. (1979): The Origin of the Makgadikgadi Pans. In: Botswana Notes and Records 11, 37–42.

Craig, H. (1957): Isotopic standards for carbon and oxygen and correction factors for mass-spectrometric analysis of carbon dioxide In: Geochimica et Cosmochimica Acta 12, 133–149. https://doi.org/10.1016/0016-7037(57)90024-8

Denffer, D. V. (1983): Morphologie. In Denffer, D.; Ziegler, H.; Ehrendorfer, F. and Bresinsky, A. (eds.): Lehrbuch der Botanik. Stuttgart.

Détienne, P. (1989): Appearance and Periodicity of Growth Rings in some Tropical Woods. In: IAWA Journal 10, 123–132. https://doi.org/10.1163/22941932-90000480

Dunwiddie, P. W. and Lamarche, V. C. J. (1980): A climatically responsive tree-ring record from *Widdringtonia cedarbergensis*, Cape Province, South Africa. In: Nature 286, 796–797. https://doi.org/10.1038/286796a0

Duquesnay, A.; Bréda, N.; Stievenard, M. and Dupouey, J. L. (1998): Changes of tree-ring $\delta^{13}C$ and water-use efficiency of beech (*Fagus sylvatica* L.) in north-eastern France during the past century. In: Plant, Cell & Environment 21, 565–572. https://doi.org/10.1046/j.1365-3040.1998.00304.x

Farquhar, G. and Lloyd, J. (1993): Carbon and oxygen isotope effects in the exchange of carbon dioxide between terrestrial plants and the atmosphere. In: Stable isotopes and plant carbon-water relations 40, 47–70.

Farquhar, G. D. and Cernusak, L. A. (2005): On the isotopic composition of leaf water in the non-steady state. In: Functional Plant Biology 32, 293–303. https://doi.org/10.1071/Fp04232

Farquhar, G. D.; O'Leary, M. H. and Berry, J. A. (1982): On the Relationship between carbon isotope discrimination and the intercellular carbon dioxide concentration in leaves. In: Australian Journal of Plant Physiology 9, 121–137. https://doi.org/10.1071/Pp9820121

Farquhar, G. D. and Sharkey, T. D. (1982): Stomatal conductance and photosynthesis. In: Annual Review of Plant Physiology 33, 317–345.

February, E. C. and Gagen, M. (2003): A dendrochronological assessment of two South African *Widdringtonia* species. In: South African Journal of Botany 69, 428–433. https://doi.org/10.1016/S0254-6299(15)30326-4

February, E. C. and Stock, W. D. (1998): An assessment of the dendro-chronological potential of two *Podocarpus* species. In: The Holocene 8, 747–754. https://doi.org/10.1191/095968398674919061

Fenner, M. (1980): Some Measurements on the water relations of Baobab trees. In: Biotropica 12, 205–209. https://doi.org/10.2307/2387972

Fichtler, E.; Trouet, V.; Beeckman, H.; Coppin, P. and Worbes, M. (2004): Climatic signals in tree rings of *Burkea africana* and *Pterocarpus angolensis* from semiarid forests in Namibia. In: Trees-Structure and Function 18, 442–451. https://doi.org/10.1007/s00468-004-0324-0

Fisher, J. B. (1981): Wound healing by exposed secondary xylem in *Adansonia* (Bombacaceae). In: IAWA Bulletin n.s. 2, 193–199. https://doi.org/10.1163/22941932-90000732

Frank, D. C.; Poulter, B.; Saurer, M.; Esper, J.; Huntingford, C.; Helle, G.; Treydte, K.; Zimmermann, N. E.; Schleser, G.; Ahlström, A.; Ciais, P.; Friedlingstein, P.; Levis, S.; Lomas, M.; Sitch, S.; Viovy, N.; Andreu-Hayles, L.; Bednarz, Z.; Berninger, F.; Boettger, T.; D'Alessandro, C. M.; Daux, V.; Filot, M.; Grabner, M.; Gutierrez, E.; Haupt, M.; Hilasvuori, E.; Jungner, H.; Kalela-Brundin, M.; Krapiec, M.; Leuenberger, M.; Loader, N. J.; Marah, H.; Masson-Delmotte, V.; Pazdur, A.; Pawelczyk, S.; Pierre, M.; Planells, O.; Pukiene, R.; Reynolds-Henne, C. E.; Rinne, K. T.; Saracino, A.; Sonninen, E.; Stievenard, M.; Switsur, V. R.; Szczepanek, M.; Szychowska-Krapiec, E.; Todaro, L.; Waterhouse, J. S. and Weigl, M. (2015): Water-use efficiency and transpiration across European forests during the Anthropocene. In: Nature Climate Change 5, 579–583. https://doi.org/10.1038/nclimate2614

Fritts, H. C. (1976): Tree Rings and Climate. London, Uk.

Gebrekirstos, A.; Van Noordwijk, M.; Neufeldt, H. and Mitlöhner, R. (2011): Relationships of stable carbon isotopes, plant water potential and growth: an approach to asses water use efficiency and growth strategies of dry land agroforestry species. In: Trees-Structure and Function 25, 95–102. https://doi.org/10.1007/s00468-010-0467-0

Gessler, A.; Ferrio, J. P.; Hommel, R.; Treydte, K.; Werner, R. A. and Monson, R. K. (2014): Stable isotopes in tree rings: towards a mechanistic understanding of isotope fractionation and mixing processes from the leaves to the wood. In: Tree Physiology 34, 796–818. https://doi.org/10.1093/treephys/tpu040

Guy, G. L. (1970): *Adansonia digitata* and its rate of growth in relation to rainfall in south central Africa. In: Proceedings and transactions – Rhodesia Scientific Association 54, 68–84.

Guy, P. R. (1982): Baobabs and elephants. In: African Journal of Ecology 20, 215–220. https://doi.org/10.1111/j.1365–2028.1982.tb00295.x

Heinrich, I. and Banks, J. C. G. (2006): Tree-ring anomlies in *Toona ciliata*. In: IAWA Journal 27, 213–231. https://doi.org/10.1163/22941932-90000150

Helle, G. and Schleser, G. H. (2004): Interpreting climate proxies from tree-rings. In Fischer, H.; Floeser, G.; Kumke, T.; Lohmann, G.; Miller, H.; Negendank, J. F. W. and Von Storch, H. (eds.): The climate in historical times: towards a synthesis of Holocene proxy data and climate models. Berlin, 129–148.

Hitchcock, R. K. and Nangati, F. M. (2000): People of the two-way river: socioeconomic change and natural resource management in the Nata River region. In: Botswana Notes and Records 32, 85–105.

Hughes, M. K. (2011): Dendroclimatology in High-Resolution Paleoclimatology. In Hughes, M. K.; Swetnem, T. W. and Diaz, H. F. (eds.): Dendroclimatology - Progress and Prospects. Dordrecht, Heidelberg, London, New York.

IPCC (2007): Climate Change 2007: Impacts, adaptions and vulnerability. Contribution of working group II to the Fourth Assessment Report of the Intergovernmental Panel on Climate Change. Cambridge.

– (2013): Climate Change 2013: The physical science basis. Contribution of Working Group I to the Fifth Assessment Report of the Intergovernmental Panel on Climate Change. Cambridge.

Laumer, W.; Andreu, L.; Helle, G.; Schleser, G. H.; Wieloch, T. and Wissel, H. (2009): A novel approach for the homogenization of cellulose to use micro-amounts for stable isotope analyses. In: Rapid Communications in Mass Spectrometry 23, 1934–1940. https://doi.org/10.1002/Rcm.4105

Livingstone, D. (1868): Missionary travels and researches in South Africa. New York.

Loader, N. J.; Robertson, I. and Mccarroll, D. (2003): Comparison of stable carbon isotope ratios in the whole wood, cellulose and lignin of oak tree-rings. In: Palaeogeography, Palaeoclimatology, Palaeoecology 196, 395–407. https://doi.org/10.1016/s0031-0182(03)00466-8

Maslin, M. A. and Christensen, B. (2007): Tectonics, orbital forcing, global climate change, and human evolution in Africa: introduction to the African paleoclimate special volume. In: Journal of Human Evolution 53, 443–464. https://doi.org/10.1016/j.jhevol.2007.06.005

Mayewski, P. A.; Rohling, E. E.; Curt Stager, J.; Karlén, W.; Maasch, K. A.; David Meeker, L.; Meyerson, E. A.; Gasse, F.; Van Kreveld, S.; Holmgren, K.; Lee-Thorp, J.; Rosqvist, G.; Rack, F.; Staubwasser, M.; Schneider, R. R. and Steig, E. J. (2004): Holocene climate variability. In: Quaternary Research 62, 243–255. https://doi.org/10.1016/j.yqres.2004.07.001

Mccarroll, D. and Loader, N. J. (2004): Stable isotopes in tree rings. In: Quaternary Science Reviews 23, 771–801. https://doi.org/10.1016/j.quascirev.2003.06.017

Neukom, R. and Gergis, J. (2012): Southern Hemisphere high-resolution palaeoclimate records of the last 2000 years. In: The Holocene 22 (5), 501–524. https://doi.org/10.1177/0959683611427335

Neukom, R.; Nash, D. J.; Endfield, G. H.; Grab, S. W.; Grove, C. A.; Kelso, C.; Vogel, C. H. and Zinke, J. (2013): Multi-proxy summer and winter precipitation reconstruction for southern Africa over the last 200 years. In: Climate Dynamics 42, 2713–2726. https://doi.org/10.1007/s00382-013-1886-6

Nicholson, S. E. and Kim, J. (1997): The relationship of the El Niño-Southern Oscillation to African rainfall. In: International Journal of Climatology 17, 117–135. https://doi.org/10.1002/(Sici)1097-0088(199702)17:2<117::Aid-Joc84>3.0.Co;2-O

Norström, E.; Holmgren, K. and Mörth, C.-M. (2008): A 600-year-long $\delta^{18}O$ record from cellulose of *Breonadia salicina* trees, South Africa. In: Dendrochronologia 26, 21–33. https://doi.org/10.1016/j.dendro.2007.08.001

Patrut, A.; Von Reden, K. F.; Mayne, D. H.; Lowy, D. A. and Patrut, R. T. (2013): AMS radiocarbon investigation of the African baobab: Searching for the oldest tree. In: Nuclear Instruments and Methods in Physics Research Section B: Beam Interactions with Materials and Atoms 294, 622–626. https://doi.org/10.1016/j.nimb.2012.04.025

Patrut, A.; Von Reden, K. F.; Pohlman, J. W.; Wittmann, R.; Mitchell, C. S.; Lowy, D. A.; Alberts, A. H.; Gerlach, D. and Xu, L. (2007): Radiocarbon dating of a very large African baobab. In: Tree Physiology 27, 1569–1574. https://doi.org/10.1093/treephys/27.11.1569

Pettigrew, J. D.; Bell, K. L.; Bhagwandin, A.; Grinan, E.; Jillani, N.; Meyer, J.; Wabuyele, E. and Vickers, C. E. (2012): Morphology, ploidy and molecular phylogenetics reveal a new diploid species from Africa in the baobab genus *Adansonia* (Malvaceae: Bombacoideae). In: Taxon 61, 1240–1250.

Pock Tsy, J. M. L.; Lumaret, R.; Mayne, D.; Vall, A. O.; Abutaba, Y. I.; Sagna, M.; Rakotondralambo Raoseta, S. O. and Danthu, P. (2009): Chloroplast DNA phylogeography suggests a West African centre of origin for the baobab, *Adansonia digitata* L. (Bombacoideae, Malvaceae). In: Molecular Ecology 18, 1707–1715. https://doi.org/10.1111/j.1365-294X.2009.04144.x

Priya, P. B. and Bhat, K. M. (1998): False ring formation in teak (*Tectona grandis* L.f.) and the influence of environmental factors. In: Forest Ecology and Management 108, 215–222. https://doi.org/10.1016/S0378-1127(98)00227-8

Rajput, K. S. (2004): Formation of unusual tissue complex in the stem of *Adansonia digitata* Linn. (Bombacaceae). In: Beiträge zur Biologie der Pflanzen 73, 331–342.

Riedel, F.; Erhardt, S.; Chauke, C.; Kossler, A.; Shemang, E. and Tarasov, P. (2012): Evidence for a permanent lake in Sua Pan (Kalahari, Botswana) during the early centuries of the last millenium indicated by distribution of Baobab trees (*Adansonia digitata*) on "Kubu Island". In: Quaternary International 253, 67–73. https://doi.org/10.1016/j.quaint.2011.02.040

Riedel, F.; Henderson, A. C. G.; Heussner, K. U.; Kaufmann, G.; Kossler, A.; Leipe, C.; Shemang, E. and Taft, L. (2014): Dynamics of a Kalahari long-lived mega-lake system: hydromorphological and limnological changes in the Makgadikgadi Basin (Botswana) during the terminal 50 ka. In: Hydrobiologia 739, 25–53. https://doi.org/10.1007/s10750-013-1647-x

Robertson, I.; Loader, N. J.; Froyd, C. A.; Zambatis, N.; Whyte, I. and Woodborne, S. (2006): The potential of the baobab (*Adansonia digitata* L.) as a proxy climate archive. In: Applied Geochemistry 21, 1674–1680. https://doi.org/10.1016/j.apgeochem.2006.07.005

Roden, J. S.; Lin, G. G. and Ehleringer, J. R. (2000): A mechanistic model for interpretation of hydrogen and oxygen isotope ratios in tree-ring cellulose. In: Geochimica et Cosmochimica Acta 64, 21–35. https://doi.org/10.1016/S0016-7037(99)00195-7

Roth-Nebelsick, A. (2006): Nach oben gezogen: Die Prinzipien der pflanzlichen Wasserleitung. In: Biologie in unserer Zeit 36, 110–118. https://doi.org/10.1002/biuz.200610305

Sano, M.; Xu, C. and Nakatsuka, T. (2012): A 300-year Vietnam hydroclimate and ENSO variability record reconstructed from tree ring$\delta^{18}O$. In: Journal of Geophysical Research: Atmospheres 117, D12115. https://doi.org/10.1029/2012jd017749

Sass, U.; Killmann, W. and Eckstein, D. (1995): Wood formation in two species of Dipterocarpaceae in Peninsular Malaysia. In: IAWA Journal 16, 371–384. https://doi.org/10.1163/22941932-90001427

Saurer, M.; Siegwolf, R. T. W. and Schweingruber, F. H. (2004): Carbon isotope discrimination indicates improving water-use efficiency of trees in northern Eurasia over the last 100 years. In: Global Change Biology 10, 2109–2120. https://doi.org/10.1111/j.1365-2486.2004.00869.x

Scheidegger, Y.; Saurer, M.; Bahn, M. and Siegwolf, R. (2000): Linking stable oxygen and carbon isotopes with stomatal conductance and photosynthetic capacity: a conceptual model. In: Oecologia 125, 350–357. https://doi.org/10.1007/s004420000466

Schollaen, K.; Heinrich, I. and Helle, G. (2014): UV-laser-based microscopic dissection of tree rings – a novel sampling tool for $\delta^{13}C$ and $\delta^{18}O$ studies. In: New Phytologist 201, 1045–1055. https://doi.org/10.1111/nph.12587

Schulman, E. (1956): Dendroclimatic changes in semiarid America. Tucson.

Schweingruber, F. H. (1983): Der Jahrring: Standort, Methodik, Zeit und Klima in der Dendrochronologie. Bern.

Seibt, U.; Rajabi, A.; Griffiths, H. and Berry, J. A. (2008): Carbon Isotopes and Water Use Efficiency: Sense and Sensitivity. In: Oecologia 155, 441–454. https://doi.org/10.1007/s00442-007-0932-7

Skomarkova, M. V.; Vaganov, E. A.; Mund, M.; Knohl, A.; Linke, P.; Boerner, A. and Schulze, E. D. (2006): Inter-annual and seasonal variability of radial growth, wood density and carbon isotope ratios in tree rings of beech (*Fagus sylvatica*) growing in Germany and Italy. In: Trees-Structure and Function 20, 571–586. https://doi.org/10.1007/s00468-006-0072-4

Sletten, H. R.; Railsback, L. B.; Liang, F.; Brook, G. A.; Marais, E.; Hardt, B. F.; Cheng, H. and Edwards, R. L. (2013): A petrographic and geochemical record of climate change over the last 4600 years from a northern Namibia stalagmite, with evidence of abruptly wetter climate at the beginning of southern Africa's Iron Age. In: Palaeogeography, Palaeoclimatology, Palaeoecology 376, 149–162. https://doi.org/10.1016/j.palaeo.2013.02.030

Spinoni, J.; Vogt, J.; Naumann, G.; Carrao, H. and Barbosa, P. (2015): Towards identifying areas at climatological risk of desertification using the Köppen-Geiger classification and Fao aridity index. In: International Journal of Climatology 35, 2210–2222. https://doi.org/10.1002/joc.4124

Stahle, D. W.; Mushove, P. T.; Cleaveland, M. K.; Roig, F. and Haynes, G. A. (1999): Management implications of annual growth rings in *Pterocarpus angolensis* from Zimbabwe. In: Forest Ecology and Management 124, 217–229. https://doi.org/10.1016/S0378-1127(99)00075-4

Swart, E. R. (1963): Age of the Baobab Tree. In: Nature 198, 708–709. https://doi.org/10.1038/198708b0

Tarhule, A. and Hughes, M. K. (2002): Tree-ring research in semi-arid West Africa: Need and potential. In: Tree-Ring Research 58, 31–46.

Therrell, M. D.; Stahle, D. W.; Ries, L. P. and Shugart, H. H. (2006): Tree-ring reconstructed rainfall variability in Zimbabwe. In: Climate Dynamics 26, 677–685. https://doi.org/10.1007/s00382-005-0108-2

Treydte, K.; Boda, S.; Graf Pannatier, E.; Fonti, P.; Frank, D.; Ullrich, B.; Saurer, M.; Siegwolf, R.; Battipaglia, G.; Werner, W. and Gessler, A. (2014): Seasonal transfer of oxygen isotopes from precipitation and soil to the tree ring: source water versus needle water enrichment. In: New Phytologist 202, 772–783. https://doi.org/10.1111/nph.12741

Treydte, K.; Esper, J. and Gärtner, H. (2004): Stabile Isotope in der Dendroklimatologie. In: Schweizerische Zeitschrift für Forstwesen 155, 222–232. https://doi.org/10.3188/szf.2004.0222

Trouet, V. and Van Oldenborgh, G. J. (2013): KNMI climate explorer: A web-based research tool for high-resolution paleoclimatology. In: Tree-Ring Research 69, 3–13. https://doi.org/10.3959/1536-1098-69.1.3

Trouet, V.; Coppin, P. and Beeckman, H. (2006): Annual growth ring patterns in *Brachystegia spiciformis* reveal influence of precipitation on tree growth. In: Biotropica 38, 375–382. https://doi.org/10.1111/j.1744-7429.2006.00155.x

Trouet, V.; Esper, J. and Beeckman, H. (2010): Climate/growth relationships of *Brachystegia spiciformis* from the miombo woodland in south central Africa. In: Dendrochronologia 28, 161–171. https://doi.org/10.1016/j.dendro.2009.10.002

Trouet, V.; Haneca, K.; Coppin, P. and Beeckman, H. (2001): Tree Ring Analysis of *Brachystegia spiciformis* and *Isoberlinia tomentosa*: Evaluation of the Enso-Signal in the Miombo Woodland of Eastern Africa. In: IAWA Journal 22, 385–399. https://doi.org/10.1163/22941932-90000384

Walter, H. and Lieth, H. (1960): Klimadiagramm-Weltatlas. Gustav Fischer Jena.

Wang, G. and Feng, X. (2012): Response of plants' water use efficiency to increasing atmospheric CO_2 concentration. In: Environmental Science & Technology 46, 8610–8620. https://doi.org/10.1021/es301323m

Wickens, G. E. (1979): The uses of the baobab (*Adansonia digitata* L.) in Africa. In Le Houérou, H. N. (ed.): Browse in Africa: The current state of knowledge. Addis Ababa.

– (1982): The Baobab: Africa's upside-down tree. In: Kew Bulletin 37, 173–209. https://doi.org/10.2307/4109961

Wickens, G. E. and Lowe, P. (2008): The Baobabs: Pachycauls of Africa, Madagascar and Australia. London.

Wieloch, T.; Helle, G.; Heinrich, I.; Voigt, M. and Schyma, P. (2011): A novel device for batch-wise isolation of α-cellulose from small-amount wholewood samples. In: Dendrochronologia 29, 115–117. https://doi.org/10.1016/j.dendro.2010.08.008

Wilson, R. T. (1988): Vital statistics of the baobab (*Adansonia digitata*). In: African Journal of Ecology 26, 197–206. https://doi.org/10.1111/j.1365-2028.1988.tb00971.x

Woodborne, S.; Hall, G.; Robertson, I.; Patrut, A.; Rouault, M.; Loader, N. J. and Hofmeyr, M. (2015): A 1000-year carbon isotope rainfall proxy record from South African Baobab trees (*Adansonia digitata* L.). In: PloS One 10, e0124202. https://doi.org/10.1371/journal.pone.0124202

Authors:

Franziska Slotta
Institute of Geological Sciences
Freie Universität Berlin
Malteserstrasse 74-100
12249 Berlin, Germany
and
GFZ – German Research Centre for Geosciences
Section 5.2 Climate Dynamics and Landscape Evolution
Telegrafenberg
14473 Potsdam, Germany
franziska.slotta@fu-berlin.de

Dr. Gerhard Helle
GFZ – German Research Centre for Geosciences
Section 5.2 Climate Dynamics and Landscape Evolution
Telegrafenberg
14473 Potsdam, Germany

Dr. Karl-Uwe Heußner
Scientific Department of the Head Office
Deutsches Archäologisches Institut
Im Dol 2-6
14195 Berlin, Germany

Prof. Dr. Elisha M. Shemang
Department of Earth and Environmental Sciences
Botswana International University of Science and Technology
Private Bag B041, Gaborone, Botswana

Prof. Dr. Frank Riedel
Institute of Geological Sciences
Freie Universität Berlin
Malteserstrasse 74-100
12249 Berlin, Germany
and
Key Laboratory of Plateau Lake Ecology and Global Change
Yunnan Normal University
No. 1 Yuhua District, Chenggong, Kunming, China